# Experimental Study on Bedload Pulses in a Steep Flume with Boulders

Tamara Ghilardi
*PhD student, Laboratory of Hydraulic Constructions (LCH), Ecole Polytechnique Fédérale de Lausanne (EPFL), Station 18, 1015 Lausanne, Switzerland. Email: tamara.ghilardi@epfl.ch*

**ABSTRACT:** In recent years, it has been observed that bedload transport fluctuates over time in steep rivers, with wide grain size distributions. This phenomenon is perceived even under constant sediment feed and water discharge. Bedload pulses are periodical and are a consequence of grain sorting. Furthermore, along with bedload transport, other parameters fluctuate in time as flow velocity and bed morphology. The influence of macro-roughness elements on these fluctuations has not been studied yet, even though it is widely accepted that the presence of large relatively immobile boulders, such as erratic blocks often present in mountain streams, has a strong impact on flow conditions and sediment transport. In the present work, the influence of the presence of these boulders on sediment transport and flow conditions is investigated with a set of laboratory experiments carried out in a 8 m long, 0.25 m wide tilting flume (analyzed slopes $S$ range between 6.7% and 13.1%). Constant sediment and water discharge were supplied into the flume at the upstream section, for tests duration reaching 250 minutes. Experiments included the use of various boulder diameters ($D$=0.075-0.125 m) and dimensionless distances between them ($\lambda/D$=2-5, where $\lambda$ is the average distance between boulders). Sediment transport, protrusion of several and bulk mean flow velocities are measured regularly during experiments. Bedload pulses or fluctuations, well-behaved periodically, are clearly visible in the measurement of sediment transport at the downstream section. Fluctuations in boulder protrusion and average velocity are also detected. Auto-correlation analysis shows that the duration of the cycles is similar for all the mentioned variables. A detailed analysis of period and amplitude of bedload transport is carried for 16 experiments with similar sediment supply. For high flow conditions, the amplitude of the bedload pulses decreases. The period and amplitude of these fluctuations is clearly related to the stream power and to the presence of boulders, considering the number of boulders and their protrusion. This article shows that for higher stream power fluctuations decrease, both in duration of a cycle and in amplitude. The presence of boulders increases the stream power needed to transport a given amount of sediments, thus decreasing fluctuations.

**KEY WORDS:** Bedload fluctuations, Pulses period and amplitude, Boulders, Steep channel, Wide grain size distribution.

## 1 INTRODUCTION

Although mountain rivers control sediment supply to lowland rivers, only relatively few studies have been made on steep mountain channels, and this mainly during the last two decades. Alpine rivers, often called gravel or boulder bed streams, are typically characterized by longitudinal slopes ranging from 0.1% to almost 20% or more (Papanicolaou et al., 2004) and a wide grain-size distribution that is composed by coarse mobile sediments and by large, relatively immobile blocks or boulders (Rickenmann, 2001; Papanicolaou et al., 2004; Yager et al., 2007). In these torrents, water depth is small when compared to roughness elements like large relatively immobile boulders, which can therefore be considered as macro-roughness elements.

The presence of a wide grain size distribution (GSD) on steep slopes has a noticeable impact on bedload. In the last decades, several researchers studied this phenomenon in experimental flumes (Iseya et al., 1987; Frey et al., 2003). Iseya et al. (1987) showed that a longitudinal sediment sorting occurs when a wide GSD is constantly fed into a flume. This segregation produces rhythmic fluctuations in the bedload transport rate. Moreover, sediment particles availability, induced by longitudinal sediment sorting, determines the magnitude of sediment transport rate and its pulses. According to Iseya et al. (1987), two main factors cause sediment transport to fluctuate. Namely migrations of bedforms and segregation of the surface grain size distribution with the formation of an armor layer. Recking et al. (2009) indicated that this phenomenon is accentuated in low flow conditions (small discharge) and is associated with fluctuations of bed slopes, bed load and bed state. Recking et al. (2008, 2009) carried out tests with uniform and wide grain size distribution on similar installation and noticed that bedload fluctuations were not observed in setups with uniform grain size distributions, confirming that fluctuations are a consequence of grain sorting in mixed sediment compositions.

Boulders, often present in mountain rivers, have rarely been taken into account in bedload transport experimental studies. Before Ghilardi et al. (2011, 2012), only Yager et al. (2007) carried out experiments on steep slopes in the presence of boulders (regularly spaced spheres and uniform bed material). Most sediment transport equations estimates bedload transport rates based on the difference between critical and total shear stress. The presence of macro-roughness elements bear a certain stress and disrupt the flow by altering the channel roughness (Yager et al., 2007). As Lenzi et al. (2006) underlined, if the roughness increases due to the number of boulders, the form drag will also increase. This implies lower shear stresses available at the bed for sediment entrainment. It is suggested (Yager et al., 2007), that only the part of the total bed shear stress (evaluated as $\tau=\rho ghS$, with $\rho$ the fluid density, $g$ the acceleration due to gravity, $h$ the water depth and $S$ the energy line slope) not acting on boulders will induce sediment transport. Hence, the presence of boulders decreases the sediment transport capacity (Ghilardi et al., 2011, 2012; Yager et al., 2007). Boulder dimensionless distance $\lambda/D$ (-), where $\lambda$ (m) is the average distance between boulders of diameter $D$ (m), and protrusion $P_{av}$ (m) are good proxies for sediment transport in mountain streams (Yager et al., 2012). A multitude of parameters may be used to take into account the presence of boulders in bed shear stress and bed resistance equations, but they generally resume to the number of boulders, their cross section, the bed area occupied by them, the distance between boulders and the drag coefficient (Bathurst, 1978; Canovaro et al., 2007; Pagliara et al., 2008; Yager et al., 2007).

Several authors pointed out the possible dependence of critical shear stress from the channel gradient (Papanicolaou et al., 2004; Lamb et al., 2008) and morphology (Church et al., 1998). Moreover, shear stress calculations need a precise knowledge of the channel hydraulics which has a high local variability. On the other hand, Bagnold's (1966) stream power (per unit width) criterion ($\omega=\rho gqS=\tau U$, with $q$ the specific discharge and $U$ the average velocity) can be approximated from gross channel properties, such as width and slope, combined with the discharge of the river. The stream power quantifies the rate of loss of energy as water flows downstream, and thus the power potentially available for performing geomorphic work (Bagnold et al., 1966; Petit el al. 2005, Ferguson, 2005; Parker et al. 2011). Bagnold proposed that bedload transport rate increases nonlinearly with stream power above a threshold or critical value of stream power. Petit et al. (2005) suggested that the critical specific stream power increases for greater bedform resistances due to the significant loss of energy available for sediment transport caused by these.

The objective of this paper is to show the relationship between sediment transport pulses and time varying boulder protrusion and average flow velocity. This is achieved through flume experiments where bedload, bed topography changes (protrusion fluctuations) and flow velocity are assessed. Results herein presented are based on the results of 15 experiments with boulders and one experiment without boulders, carried out for a similar average sediment transport rates. The duration and amplitude of pulses in sediment transport are analyzed as a function of discharge, bed shear stress, stream power and density of boulders. Following this introduction, the experimental methods are presented, then results are analyzed and discussed and finally main conclusions are drawn. In the presentation and discussion of results, one single experiment is described and analyzed in detail. Then, the same analysis is applied to the remaining experiments and a joint discussion of the results is given.

## 2 RESEARCH METHODS

The main goal of this research project is to analyze the impact that randomly distributed and relatively immobile boulders have on sediment transport in steep slope rivers. This is done by means of mobile bed laboratory experiments on a 8 m long (7 m usable), 0.25 m wide, tilting flume (Figure 1) at the Laboratory of Hydraulic Constructions (LCH) at the Ecole Polytechnique Fédérale de Lausanne (EPFL).

Water discharge, fed constantly by the closed general pumping system of the laboratory, is measured by an electromagnetic flow-meter. Sediments are constantly fed into the system by a calibrated sediment feeder situated upstream. A filtering basket suspended to a balance recuperates the sediments at the outlet, where the weight is measured every minute. Knowing the precise time and amount of sediment, an average value of the sediment discharge is then calculated continuously over a sliding 10 minutes window ($q_{s,out,10'}$), in order to have a smoothed overview of the bedload fluctuations. When the sediment feeder is empty or the basket is full, the latter is emptied into the first and sediments are recirculated. No sediment sorting was observed at the outlet of the feeder. The protrusion $P$ of 4 boulders is measured with a point gauge during experiments, with a time interval of approximately 10 minutes (2-3 minutes per boulder, in a loop). $P$ is calculated as the averaged height differences between: top-upstream, top-downstream, top-left, and top-right, for every boulder at the edge with the gravel. A sub-sampled linear interpolation in time allows then the averaging between boulders with a regular time-step, originating the value of $P_{av}$, the average boulder protrusion, at every minute of the test. Flow average velocity was measured every 15 minutes by means of a technique using dye-tracer and video analysis. This technique, based on the analysis of a colorant (tracer) dilution, allows the measurement of mean bulk velocities through the channel reach. The passage of the cloud of colorant in the reach in analyzed based on the difference between images, the movement of mass center of the cloud defining the average flow velocity (cf. Calkins et al., 1970). Five colorant injections are done in order to obtain a velocity value.

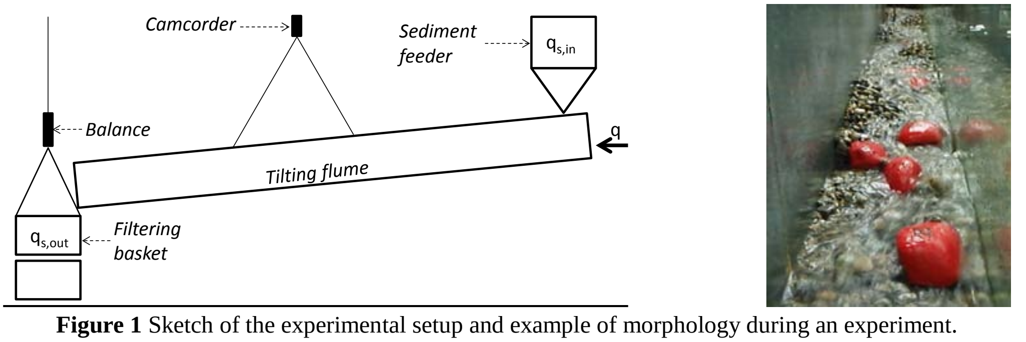


**Figure 1** Sketch of the experimental setup and example of morphology during an experiment.

The grain size distribution of the supplied sediments is: $d_m$=$d_{65}$=11.9 mm, $d_{30}$=7.1 mm, $d_{90}$=19 mm, where $d_m$ is the mean grain size, assumed equal to $d_{65}$, and $d_x$ is the grain size diameter for which $x$% in weight of the amount of sediments have smaller diameters. Boulders are not taken into account in this calculation and are not supplied as mobile sediments; they are instead placed in the bed before the experiments. Boulders are relatively immobile, which means that they are not transported by the flow, although they may move up to several times their diameter during experiments, due mainly to the erosion around them. This happens especially for the smallest diameters of boulders ($D$=0.075 m). Flume slopes, $S$, of 6.7%, 9.9% and 13% were tested. Boulders of diameters, $D$, of 0.075 m, 0.100 m and 0.125 m were randomly placed into the flume with a dimensionless distance $\lambda/D$ of 2, 3 and 5. In the present article 16 configurations are tested and analyzed in the next section. For a given boulder configuration $\lambda/D$-$D$, the initial position of the boulders is always the same.

A plane bed is prepared before the experiments and boulders are placed into the flume half covered by mobile sediments, which corresponds to a protrusion equal to approximately 30% of the diameter ($P^*$=$P_{av}/D$≈0.3). Water and sediment supply are started at the same time. During the experiment flow velocity $U$ is measured every 15 minutes and the protrusion of 4 boulders is measured in a loop. Average velocity $U$ and boulder protrusion $P_{av}$ are sub-sampled, by linear interpolation, in order to have a regular interval of 1 minute, the same measuring period used for sediment transport $q_{s,out,10'}$.

The equilibrium condition between liquid and solid discharge has to be such that boulders are still relatively visible at the end of the experiment. The test is stopped immediately after a peak in bedload, when the average outlet sediment discharge over the last 10 minutes is equal to the sediment supply ($q_{s,out,10'} \approx q_{s,in}$). The overall cumulative average of the outlet sediment transport computed for a given instant T ($q_{s,out,av}$, Eq.(1)) has to be within ±15% of the sediment supply at the end of the experiment.

$$q_{s,out,av}(T) = \left( \int_0^T q_{s,out}(t)\,\mathrm{d}t \right) \Big/ T \qquad (1)$$

## 3 RESULTS AND DISCUSSION

### 3.1 Detailed analysis of one experimental test

#### 3.1.1 Time series analysis

Pulses in bedload ($q_{s,out,10'}$) coupled with cyclic changes in boulder protrusion ($P_{av}$) and average flow velocity ($U$), were observed in all the experiments. The duration and amplitude of these pulses varies between the tests.

Figure 2 presents time series of bedload (with sampling period of 1 minute), boulder average protrusion (with sampling period of 2-3 minutes per boulder, for a total of 3-4 boulders, in a loop, depending on the test), and mean flow velocities (with sampling period of 15 minutes). In this, coupled fluctuations of $q_{s,out,10'}$, $P_{av}$ and $U$ are clearly visible. Three peaks in sediment transport $q_{s,out,10'}$ and average dimensionless boulder protrusion $P^*$ (calculated by scaling the measured instantaneous averaged protrusion $P_{av}$ in meters, with the boulder diameter $D$: $P^*=P_{av}/D$) are clearly visible. The interval between occurrences of these peaks is approximately 80 minutes. Despite the low measuring resolution, two peaks are identified in average flow velocity $U$ for this experiment, corresponding always to high sediment transport values.

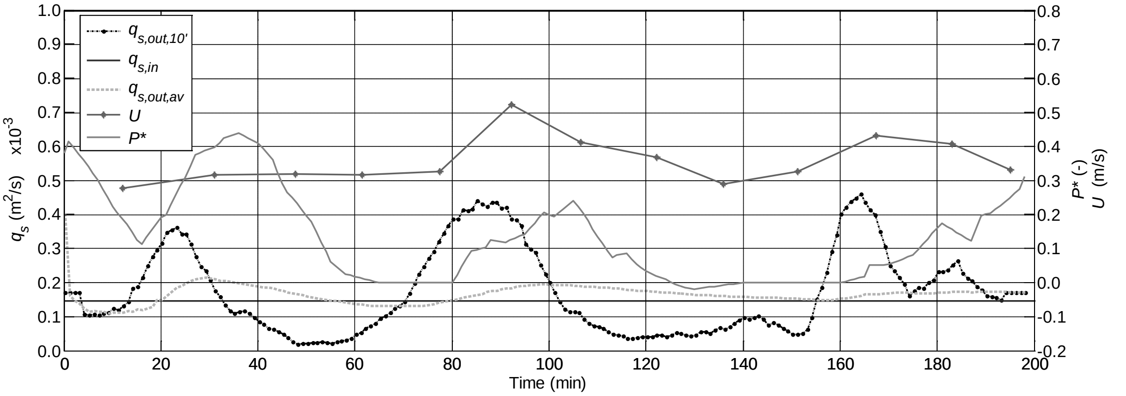


**Figure 2** Time series of measured of bedload averaged over a 10 minutes window ($q_{s,out,10'}$), sediment supply ($q_{s,in}$) and global outlet ($q_{s,out,av}$) on the left axis. Time series of measured of mean velocity ($U$) and dimensionless average protrusion ($P^*$), calculated as instantaneous mean protrusion ($P_{av}$) divided by mean boulder diameter ($D$), on the right axis. The time indicates the duration from the beginning of the experiment. The dots in the velocity curve indicate the points actually measured. Test with $N_{Bs}$=20 m$^{-2}$ boulders of diameter $D$=0.075 m, $\lambda/D$=3, $q_{s,in}$=0.146 x10$^{-3}$ m$^2$/s, $q$= 0.0109 m$^2$/s and $S$=13.0%.

Unit bedload transport varies from a minimum of 0.018 x10$^{-3}$ m$^2$/s to a maximum of 0.460 x10$^{-3}$ m$^2$/s, with an average value of 0.172 x10$^{-3}$ m$^2$/s and a standard deviation of 0.125 x10$^{-3}$ m$^2$/s, corresponding to 72% of the average.

Boulder protrusion $P^*$ also presents ample fluctuations, ranging from a minimum of -0.02, where the boulders are visible although the gravel deposited around the boulder is higher than the boulder top, to a maximum of 0.44, where the boulders are almost completely exposed to the flow. The average protrusion through the experiment is 0.13 and the standard deviation is 0.13. Sediment transport starts to increase when boulder protrusion is at its minimum, equal or close to zero. Protrusions reaches its maximum at the end of a sediment transport peak, when the average bedload outlet over 10 minutes ($q_{s,out,10'}$) corresponds to the inlet ($q_{s,in}$) and is followed by a period where sediment transport is below $q_{s,in}$. This result confirms the observation made by Yager et al. (2012), stating that boulder protrusion $P^*$ is a good proxy for sediment transport in time, since it continuously varies in phase with sediment transport in time, for a given reach.

Fluctuations in flow velocities $U$ are smaller. Peaks in velocity occur almost at the same time as the peak in sediment transport. It is likely that a peak in average flow velocity should occur around 20 minutes, but the velocity measurement interval, which is of 15 minutes, did not allow capturing it.

### 3.1.2 Auto-correlation functions

Figure 3 presents normalized auto-correlation function of $q_{s,out,10'}$, $U$ and $P^*$, according to Figure 2. The first meaningful peak in the auto-correlation function corresponding to the sediment transport occurs at a time lag of 76 minutes. This time lag corresponds roughly to the period identified early for bedload pulses of about 80 minutes (cf. Figure 2). A second peak in the auto-correlation function for the sediment transport is seen for a time lag of around 142 minutes about two times the time lag of the first peak, corroborating this as a good estimation for the duration of the fluctuations.

The shape of protrusion and average velocities auto-correlation functions, variables with less time resolution given the experimental procedure followed, indicate as expected cyclic behavior of the time series similar to the sediment transport. Due to the duration of the experiment (200 minutes) and the duration of a cycle (only three captured in this long experimental run), only the first correlational peaks are statistically relevant. Nevertheless, their coincidence and clarity confer meaningfulness to the above observations.

Visual observation of the experiments and video recordings show that the observed sediment transport fluctuations correspond to different bed states. During low sediment transport event, an aggradation of the bed is observed, associated with vertical grain sorting. Fine sediments are visible in the subsurface while a layer of one to two very coarse grains is present on the surface. Steep riffles can form locally, especially when few boulders are present. The slope of the riffle slowly increases until a maximum, flow accelerates and eventually the structure fails allowing the mobilization of fine sediments initially trapped in the subsurface layer. Once a new equilibrium between bedforms, slope and surface grain size is found, a new cycle of bed aggradation that will be followed by destruction starts. A more detailed description and discussion on bedforms migration and destruction, causing bedload pulses, can be found in Ghilardi et al. (2013).

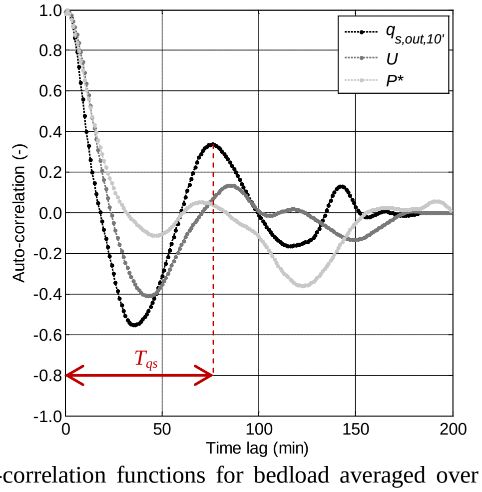


**Figure 3** Normalized auto-correlation functions for bedload averaged over a 10 minutes window ($q_{s,out,10'}$), mean velocity ($U$) and dimensionless average protrusion ($P^*$). Test with $N_{Bs}$=20 $m^{-2}$ boulders of diameter $D$=0.075 m, $\lambda/D$=3, $q_{s,in}$=0.146 x$10^{-3}$ $m^2$/s, $q$= 0.0109 $m^2$/s and $S$=13.0%. $T_{qs}$ indicates the time lag used to define the duration of a bedload cycle.

### 3.2 Bedload pulses characterization: amplitude and period

The cyclic fluctuations described above and clearly shown in Figure 2 and Figure 3 were observed in all the experiments. 15 other experiments, carried out with similar sediment supply ($q_{s,in}$=0.135 x$10^{-3}$ $m^2$/s for $S$=6.7% and $S$=9.9% ; $q_{s,in}$=0.151 x$10^{-3}$ $m^2$/s for $S$=13%), are used further to investigate bedload pulses in steep slopes in the presence of large-scale boulders. For this analysis, two parameters characterizing the fluctuating behavior of the sediment transport for each test are used: duration ($T_{qs}$) and amplitude ($\sigma_{qs}/q_{s,out,av}$). The duration of the fluctuation of sediment transport $T_{qs}$ is defined as the time lag of the first peak in the auto-correlation function (cf. Figure 3). The amplitude of the fluctuations is defined as the standard deviation on bedload $\sigma_{qs}$ divided by the average sediment transport $q_{s,out,av}$ ($\sigma_{qs}/q_{s,out,av}$).

Table 1 presents the configuration of the experiments used for the analysis, characterized by the slope $S$, the dimensionless boulder distance $\lambda/D$, boulder diameter $D$, number of boulder per square meter $N_{Bs}$ and water discharge $q$, as well as the main results, such as mean water depth $h_{calc}$, average sediment outlet $q_{s,out,av}$, bedload standard deviation $\sigma_{qs}$, the period of bedload fluctuations $T_{qs}$, the normalized bedload amplitude $\sigma_{qs}/q_{s,out,av}$ and $P_{\overline{av}}$ the average of the average boulder protrusion ($P_{av}$) during the whole experiment.

The standard deviation of the fluctuations ranges between 13%, for the smallest slope, and 97%, for the largest slope, of the average sediment transport during the test while the duration of fluctuations varies between 9 (slope of 6.7%) and 163 minutes (slope of 13%), for a similar sediment inlet. The water discharge needed to transport the sediments varied between 0.0391 $m^2$/s, for the experiment with the larger amount of boulders ($\lambda/D$=2, $D$=0.075 m) and the smallest slope, and 0.0104 $m^2$/s, for the smallest amount of boulders used on the steeper slope. Mean water depth $h_{calc}$, ranges from 0.027 m to 0.053 m.

**Table 1** Experimental parameters, where $S$ is the slope, $\lambda/D$ the dimensionless distance between boulders, $D$ the boulder diameter, $N_{Bs}$ the average number of boulders per square meter, q the liquid discharge; and experimental results where $h_{calc}$ is the mean water depth calculated as $h_{calc}=q/U_{\overline{av}}$ where $U_{\overline{av}}$ is the average flow velocity, $q_{s,out,av}$ the average outlet discharge, $\sigma_{qs}$ the standard deviation of the bedload, $T_{qs}$ the time lag for the first auto-correlation peak (cf. Figure 3), $\sigma_{qs}/q_{s,out,av}$ the normalized amplitude of bedload fluctuations and $P_{\overline{av}}$ the average of the average boulder protrusion ($P_{av}$) through the experiments. The symbols used to represent the experiments in Figure 4 to Figure 8 are given in the last column of the table. The shape of the symbols depends on $\lambda/D$, the filling on $D$ and the contour line color on the flume slope $S$. The line in bold presents the test described in detail in section 3.1.

| $S$ (%) | $\lambda/D$ (-) | $D$ (m) | $N_{Bs}$ ($m^{-2}$) | $q$ ($m^2$/s) | $h_{calc}$ (m) | $q_{s,out,av}$ x$10^{-3}$ ($m^2$/s) | $\sigma_{qs}$ x$10^{-3}$ ($m^2$/s) | $T_{qs}$ (min) | $\sigma_{qs}/q_{s,out,av}$ | $P_{\overline{av}}$ (m) | Symbol |
|---|---|---|---|---|---|---|---|---|---|---|---|
| 6.7 | 5 | 0.100 | 4.0 | 0.0223 | 0.039 | 0.135 | 0.037 | 85 | 0.27 | 0.046 | ■ |
| 6.7 | 5 | 0.075 | 6.9 | 0.0227 | 0.038 | 0.131 | 0.048 | 34 | 0.36 | 0.029 | ■ |
| 6.7 | 5 | 0.125 | 2.3 | 0.0208 | 0.033 | 0.150 | 0.056 | 84 | 0.37 | 0.061 | □ |
| 6.7 | 3 | 0.075 | 20.0 | 0.0238 | 0.034 | 0.140 | 0.034 | 23 | 0.24 | 0.033 | ▲ |
| 6.7 | 3 | 0.125 | 6.9 | 0.0235 | 0.039 | 0.119 | 0.036 | 23 | 0.30 | 0.054 | △ |
| 6.7 | 3 | 0.100 | 10.9 | 0.0233 | 0.043 | 0.124 | 0.034 | 21 | 0.27 | 0.031 | ▲ |
| 6.7 | 0 | 0.000 | 0.0 | 0.0162 | 0.033 | 0.119 | 0.046 | 51 | 0.39 | 0.000 | ● |
| 6.7 | 2 | 0.100 | 25.1 | 0.0372 | 0.053 | 0.139 | 0.019 | 9 | 0.14 | 0.029 | ◆ |
| 6.7 | 2 | 0.125 | 16.0 | 0.0352 | 0.050 | 0.137 | 0.018 | 14 | 0.13 | 0.040 | ◇ |
| 6.7 | 2 | 0.075 | 44.6 | 0.0391 | 0.051 | 0.146 | 0.028 | 10 | 0.19 | 0.027 | ◆ |
| 9.9 | 3 | 0.100 | 10.9 | 0.0146 | 0.027 | 0.143 | 0.053 | 18 | 0.37 | 0.035 | ▲ |
| 13.0 | 3 | 0.100 | 10.9 | 0.0107 | 0.039 | 0.145 | 0.140 | 163 | 0.97 | 0.016 | ▲ |
| **13.0** | **3** | **0.075** | **20.0** | **0.0109** | **0.030** | **0.172** | **0.125** | **76** | **0.72** | **0.010** | ▲ |
| 13.0 | 2 | 0.100 | 25.1 | 0.0128 | 0.031 | 0.168 | 0.038 | 14 | 0.23 | 0.017 | ◆ |
| 13.0 | 5 | 0.100 | 4.0 | 0.0104 | 0.028 | 0.168 | 0.074 | 68 | 0.44 | 0.024 | ■ |
| 13.0 | 3 | 0.125 | 6.9 | 0.0104 | 0.039 | 0.165 | 0.098 | 112 | 0.60 | 0.035 | △ |

In Figure 4, duration and normalized amplitude of bedload fluctuations (column 9 and 10 in Table 1, respectively) are represented as a function of the liquid discharge provided constantly during the tests. A clear link between the liquid discharge $q$ and the fluctuations in sediment transport, both in period $T_{qs}$ (Figure 4a) and in amplitude (Figure 4b), is observed. For high flow conditions (high $q$), the fluctuations are smaller in time and amplitude. For a similar sediment transport and a given slope, the discharge needed for equilibrium conditions is generally higher for smaller $\lambda/D$. The tests are clearly grouped as a function of the slope. As stated by bedload transport formulae (Rickenmann et al., 2001; Recking, 2006; Yager et al. 2007; Ghilardi et al. 2011), the discharge for equilibrium sediment transport is higher on lower slopes.

In Figure 5 bedload fluctuation characteristics, duration and amplitude, are plotted against each other. When the duration of a cycle is long, its amplitude is also large, as shown on Figure 5. This is explained by the fact that in longer cycles, the duration of low sediment transport is extended. A considerable amount of gravel is thus accumulated in the flume and, since the sediment transport is similar, it directly depends on the duration. When coarse structures are destroyed, a large amount of underlaying fine sediments is freed and contributes to the peak in sediment transport (Ghilardi et al. 2013), which will thus have a larger amplitude.

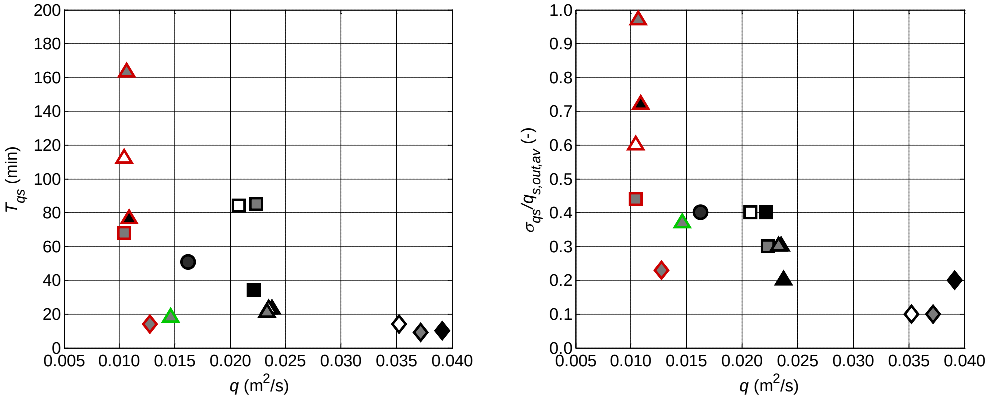


**Figure 4** (a) Duration $T_{qs}$ and (b) amplitude $\sigma_{qs}/ q_{s,out,av}$ of bedload fluctuations as a function of water discharge. Symbols used are presented in Table 1.

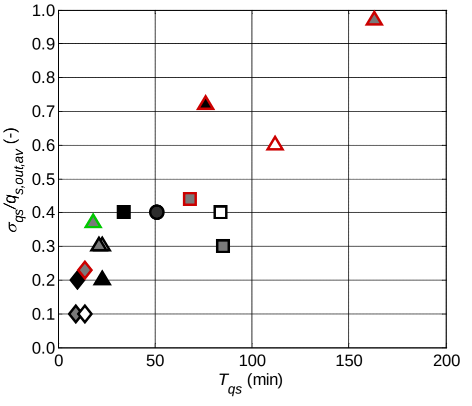


**Figure 5** Relation between duration $T_{qs}$ and amplitude $\sigma_{qs}/q_{s,out,av}$ of bedload fluctuations. Symbols used are presented in Table 1.

In Figure 6 characteristics of bedload fluctuations, duration and amplitude, are plotted against the bed shear stress, which is calculated as $\tau=\rho ghS$. Assuming a uniform flow, the flume slope $S$ is used instead of the energy slope, which can be accepted on a reach average. The bed shear stress is larger on higher slopes. Although the fluctuations amplitude (Figure 6b) tend to be smaller for lower shear stresses, no clear trend of the fluctuation period (Figure 6a) can be identified. Thus, bed shear stress does not seem relevant to quantify fluctuations in bedload.

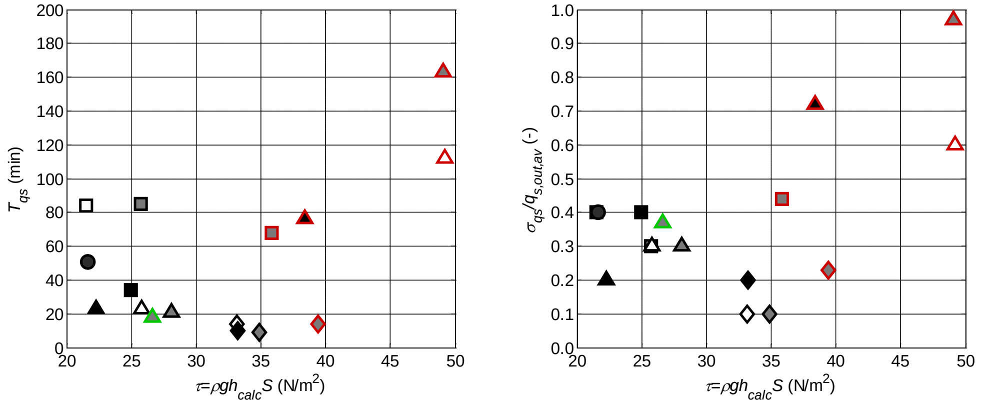


(a) (b)

**Figure 6** (a) Duration $T_{qs}$ and (b) amplitude $\sigma_{qs}/ q_{s,out,av}$ of bedload fluctuations as a function of bed shear stress $\tau$. Symbols used are presented in Table 1.

Stream power is widely used to characterize sediment transport. The clear separation of experiments by slope, and the clear trend of duration and amplitude of bedload cycles as function of the discharge presented in Figure 4, suggests a link between bedload fluctuations and the stream power $\omega=\rho gqS=\tau \bar{U}_{av}$, which represents the rate of loss of energy as water flows downstream. This is clearly shown in Figure 7, where bedload fluctuation characteristics, duration and amplitude, are plotted against stream power. Duration and amplitude of the fluctuations decreases when the stream power increases. For higher stream power no grain sorting was observed during the experiments. This is likely due to the higher energy available to transport all the mobile sediment diameters. The absence of vertical sorting does not allow the creation and destruction of coarse riffles, which is causing bedload fuctuations (cf. §3.1 and Ghilardi et al., 2012, 2013). The attenuation of fluctuations is fast at first (increase in small stream power), but quickly reaches a lower limit for a stream power around 15-20 W/m$^2$. For experiments carried out on small slopes the stream power is generally higher. The stream power is especially high for tests with $\lambda/D$=2 on the 6.7% slope. For these tests the water discharge was much greater than for other tests, due to the energy dissipated by the large number of boulders present and their protrusion from the mobile sediments. Figure 6 and Figure 7 undoubtfully show that the potential energy available to the stream ($\omega$), and not the forces available ($\tau$), characterize the amplitude and duration of bedload pulses, and thus morphological changes, as indicated by Figure 2.

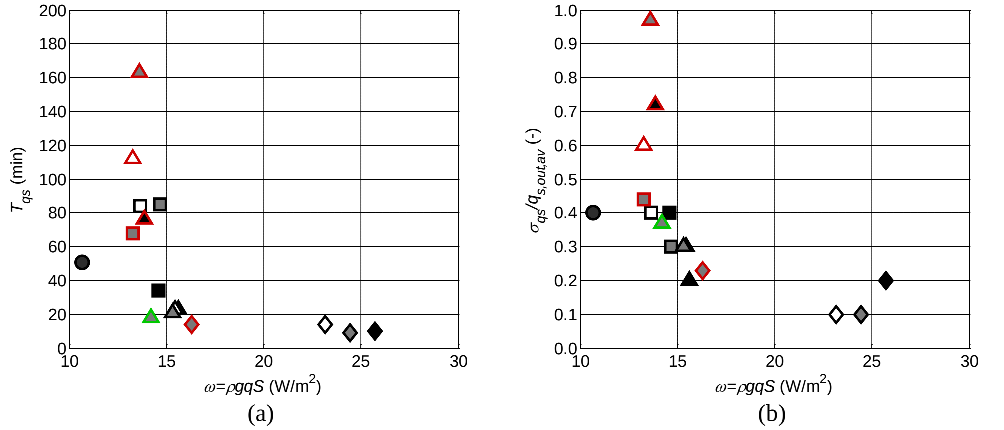


(a) (b)

**Figure 7** (a) Duration $T_{qs}$ and (b) amplitude $\sigma_{qs}/ q_{s,out,av}$ of bedload fluctuations as a function of stream power $\omega$. Symbols used are presented in Table 1.

In Figure 8 the stream power is plotted against the surface occupied by boulders, represented by $\bar{P}_{av}^{2} N_{Bs}$. A linear relation between these variables is observed. Keeping in mind that the presented tests have a similar bedload transport capacity, Figure 8 clearly shows that a higher stream power is needed for a high value of $\overline{P_{av}}^2 N_{Bs}$, which occurs for the highest spacial density of boulders ($\lambda/D$=2). This behavior underlines the important role of the energy loss due to the presence of boulders. However boulder protrusion alone cannot explain bedload fluctuations characterization. The number of roughness elements, represented by the number of boulders, have to be taken into account in order to explain the rate of total energy losses $\omega$.

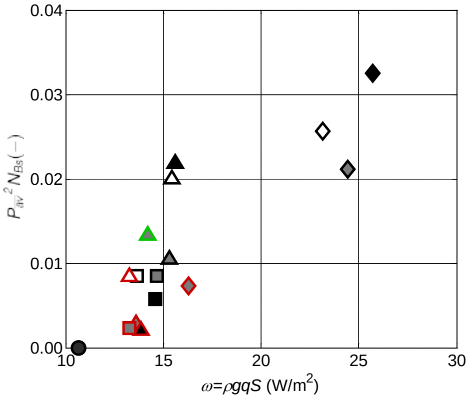


**Figure 8** Squared average protrusion $\overline{P_{av}}^2$ multiplied by the average number of boulders per square meter $N_{Bs}$ as a function of stream power $\omega$. Symbols used are presented in Table 1.

In Figure 9 bedload fluctuation characteristics, duration and amplitude, are plotted against the surface occupied by boulders, represented by $\overline{P_{av}}^2 N_{Bs}$. It is obvious that bedload fluctuations period and amplitude decrease with $\overline{P_{av}}^2 N_{Bs}$ increase, confirming that the presence of boulders stabilizes the bed, because less changes in morphology would be encountered (cf. § 3.1). This is also confirmed by the fact that the stream power needed to transport the sediments is higher. The presence of bedforms or macro-roughness elements creates significant energy losses, thus decreasing the amount of energy available to mobilize and transport sediments (Petit et al., 2005; Yager et al., 2007, 2012; Ghilardi et al., 2011, 2012).

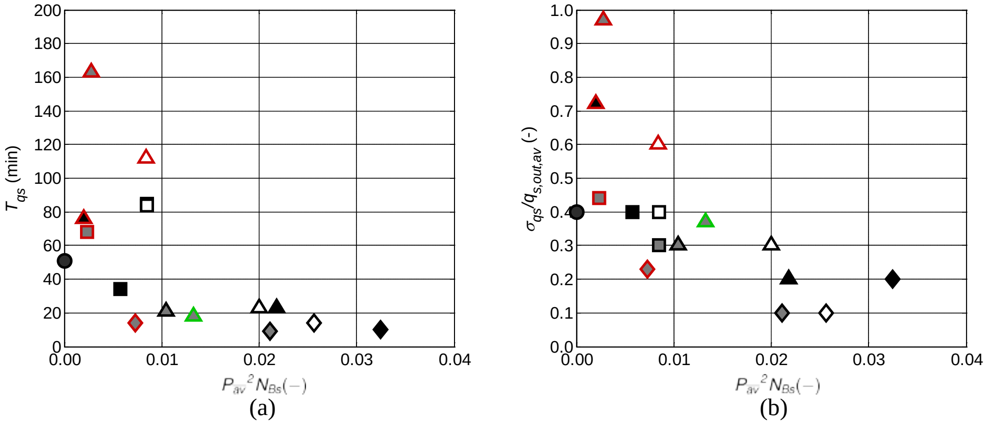


**Figure 9** (a) Duration $T_{qs}$ and (b) amplitude $\sigma_{qs}/ q_{s,out,av}$ of bedload fluctuations as a function of squared average protrusion $\overline{P_{av}}^2$, multiplied by the average number of boulders per square meter $N_{Bs}$. Symbols used are presented in Table 1.

## 4 CONCLUSION

The amplitude and period of bedload fluctuations have been analyzed through a dataset of 16 experiments carried out with varying flume slopes and boulder configuration ($\lambda/D$-$D$) for a similar sediment supply. Although these fluctuations are caused by the presence of graded bed materials and not by macro-roughness elements, the presence of boulders does have an impact on sediment transport capacity, and thus on the duration and amplitude of bedload fluctuations. At high flow conditions, sediment transport fluctuations decrease both in time and amplitude. A higher discharge is needed in order to transport the sediments when numerous boulders are present in the flume.

Bedload fluctuations characteristics are influenced both by the water discharge and by the slope. The amplitude and period of bedload pulses clearly decreases with an increase in stream power, which takes into account both the abovementioned parameters. A direct relation between the stream power and the presence of boulders, taken into account by means of number of boulders and their protrusion ( $P_{av}^{-2} N_{Bs}$ ), could be found. This proves that the energy losses caused by the boulders have an influence both on sediment transport capacity and bedload pulses characteristics (period and amplitude). The decrease in period and amplitude of bedload pulses, caused by the increase in energy losses, decreases morphological changes through time.


## ACKNOWLEDGMENTS

The present study is financed by the Swiss Competence Center for Environmental Sustainability (CCES) of the ETH domain and the Swiss Federal Office of Energy (SFOE).


**References**


Bagnold, R., 1966. An approach to the sediment transport problem from general physics. US Geol. Surv. Prof. Paper, 422, 231-291.

Bathurst, J.C., 1978. Flow resistance of large-scale roughness. Journal of hydraulics division - Proceedings of the American Society of Civil Engineers, 104 (HY12), 1587-1603.

Calkins, D., Dunne, T., 1970. A salt tracing method for measuring channel velocities in small mountain streams. Journal of Hydrology, 11, 379-392.

Canovaro, F., Paris, E., Solari, L., 2007. Effects of macro-scale bed roughness geometry on flow resistance. Water Resources Research, 43 W10414, doi:10.1029/2006 WR005727.

Church, M., Hassan, M.A., Wolcott, J.F., 1998. Stabilising self-organised structures in gravel-bed streams. Water Resources Research, 34, 3169–3179.

Ferguson, R.I., 2005. Estimating critical stream power for bedload transport calculations in gravel-bed rivers. Geomorphology, 70, 33-41.

Frey, P., Ducottet, C., Jay, J., 2003. Fluctuations of bed load solid discharge and grain size distribution on steep slopes with image analysis. Experiments in Fluids, 35, 589-597.

Ghilardi, T., Schleiss, A. J., 2011. Influence of immobile boulders on bedload transport in a steep flume. Proc. of 34th IAHR World Congress, 26 June - 1st July 2011, Brisbane, Australia, CD-Rom, ISBN 978-0-85825-868-6, 3473-3480.

Ghilardi, T., Schleiss, A.J., 2012. Steep flume experiments with large immobile boulders and wide grain size distribution as encountered in alpine torrents. Proc. of River Flow 2012, 5-7 September 2012, San José, Costa Rica, ISBN:978-1-4665-7551-6, 407-414.

Ghilardi, T., Franca, M.J., Schleiss, A.J., 2013. Temporal evolution of bedload in a steep channel over a long duration experiment. *Submitted to* the 35th IAHR World Congress, 8-13 September 2013, Chengdu, China.

Iseya, F., Ikeda, H., 1987. Pulsations in bedload transport rates induced by a longitudinal sediment sorting: A flume study using sand and gravel mixtures. Geografiska Annaler (A) 69, 15-27.

Lamb, M.P., Dietrich, W.E., Venditti, J.G., 2008. Is the critical Shields stress for incipient sediment motion dependent on channel-bed slope? Journal of Geophysical Research, 113, F02008, doi:10.1029/2007JF000831

Lenzi M.A., Mao L., Comiti F., 2006. When does bedload transport begin in steep boulder-bed streams? Hydrological Processes, 20, 3517-3533.

Pagliara, S., Das, R., Carnacina, I., 2008. Flow resistance in large-scale roughness condition. Canadian Journal of Civil Engineering, 35(11), 1285-1293.

Papanicolaou, A.N., Bdour, A., Wicklein, E., 2004. One-dimensional hydrodynamic/sediment transport model applicable to steep mountain streams. Journal of Hydraulic Research, 42 (4), 357-375.

Parker, C., Clifford, N.J., Thorne, C.R, 2011. Understanding the influence of slope on the threshold of coarse grain motion: Revisiting critical stream power. Geomorphology, 126, 51-65.

Petit, F., Gob, F., Houbrechts, G., Assani, A.A., 2005. Critical specific stream power in gravel-bed rivers. Geomorphology, 69, 92-101.

Recking, A., Frey, P., Paquier, A., Belleudy, P., Champagne, J.Y., 2008. Bedload transport flume experiments on steep slopes. Journal of Hydraulic Engineering, 134, 1302-1310.

Recking, A., Frey, P., Paquier, A., Belleudy P., 2009. An experimental investigation of mechanisms involved in bed load sheet production and migration. Journal of Geophysical Research, 114, F03010, doi:10.1029/2008JF000990

Rickenmann, D., 2001. Comparison of bed load transport in torrents and gravel bed streams. Water Resources Research, 37 (12), 3295-3305.

Yager, E.M., Kirchner, J.W., Dietrich, W.E., 2007. Calculating bed load transport in steep boulder bed channels. Water Resources Research, 43, W07418, doi:10.1029/2006 WR005432.

Yager, E.M., Turowski, J.M., Rickenman, D., McArdell, B.W., 2012. Sediment supply, grain protrusion, and bedload transport in mountain streams. Geophysical Research Letters, 39, L10402, doi:10.1029/2012GL051654